

Phosphorus–Nitrogen Compounds. Part 13. Syntheses, Crystal Structures, Spectroscopic, Stereogenic, and Anisochronic Properties of Novel Spiro-Ansa-Spiro-, Spiro-Bino-Spiro-, and Spiro-Crypta Phosphazene Derivatives

Selen Bilge, Şemsay Demiriz, Aytuğ Okumuş, and Zeynel Kılıç*

Department of Chemistry, Ankara University, 06100 Tandoğan-Ankara, Turkey

Barış Tercan and Tuncer Hökelek

Department of Physics, Hacettepe University, 06800 Beytepe-Ankara, Turkey

Orhan Büyükgüngör

Department of Physics, Ondokuz Mayıs University, 55139 Kurupelit-Samsun, Turkey

Received April 13, 2006

The condensation reactions of N_2O_x ($x = 2, 3$) donor-type aminopodand (**4**) and dibenzo-diaza-crown ethers (**5**, **6**, and **9**) with hexachlorocyclotriphosphazatriene, $N_3P_3Cl_6$, produce two kinds of partially substituted novel phosphazene derivatives, namely, spiro-bino-spiro- (**19**) and spiro-crypta (**21**, **22**, and **25**) phosphazenes. The partially substituted spiro-ansa-spiro-phosphazene (**11**) reacted with pyrrolidine and 1,4-dioxo-8-azaspiro[4,5]decane (DASD) give the corresponding new fully substituted phosphazenes (**14** and **16**). Unexpectedly, the reactions of **23** and **24** with pyrrolidine result in only *geminal* crypta phosphazenes (**26** and **27**). The solid-state structures of **16** and **22** have been determined by X-ray diffraction techniques. The relative inner hole-size of the macrocycle in the radii of **22** is 1.27 Å. The relationship between the exocyclic NPN (α') and endocyclic (α) bond angles for spiro-crypta phosphazenes and exocyclic OPN (α') bond angles for spiro-ansa-spiro- and spiro-bino-spiro-phosphazenes with ^{31}P NMR chemical shifts of NPN and OPN phosphorus atoms, respectively, have been investigated. The structures of **10**, **14**, **16**, **19**, **21**, **22**, and **25–27** have also been examined by FTIR, 1H , ^{13}C , and ^{31}P NMR, HETCOR, MS, and elemental analyses. The ^{31}P NMR spectra of **10**, **21**, **22**, and **25** indicate that the compounds have anisochrony. In compounds **16** and **22**, the spirocyclic nitrogen atoms have pyramidal geometries resulting in stereogenic properties.

Introduction

$N_3P_3Cl_6$ is known as the standard compound in the field of phosphazene chemistry. It has been used in the preparation of novel phosphazene derivatives with different substituents which are very effective in determining the physical and chemical properties of new phosphazene compounds. For several reasons, cyclophosphazenes have continued to attract the increased attention of researchers in recent years. One area of interest has focused on the replacement reactions of the halogen atom or atoms of halophosphazenes by different

nucleophiles. The reactions of $N_3P_3Cl_6$ with nucleophilic reagents, such as primary and secondary amines,¹ polyamines,² aliphatic and aromatic diols and diamines,³ and oligoethylene

- (1) (a) Fincham, J. K.; Hursthouse, M. B.; Parker, H. G.; Shaw (née Gözen), L. S.; Shaw, R. A. *J. Chem. Soc., Dalton Trans.* **1988**, 1169–1178. (b) Allen, C. W. *Chem. Rev.* **1991**, *91*, 119–135. (c) Contractor, S. R.; Kılıç, Z.; Shaw, R. A. *J. Chem. Soc., Dalton Trans.* **1987**, 2023–2029. (d) Deutch, W. F.; Hursthouse, M. B.; Kılıç, Z.; Parkers, H. G.; Shaw (née Gözen), L. S.; Shaw, R. A. *Phosphorus Sulfur Relat. Elem.* **1987**, *32*, 81–85. (e) Shaw, R. A. *Pure Appl. Chem.* **1980**, *52*, 1063–1097. (f) Krishnamurthy, S. S.; Sau, A. C.; Woods, M. In *Advances in Inorganic Chemistry and Radiochemistry*, Vol. 21; Emeleus, H. J., Ed.; Academic Press: New York, 1978; p 41. (g) Allcock, H. R. *Chem. Rev.* **1972**, *72*, 315–356. (h) Begeç, S.; Alataş, S.; Kılıç, A. *Heteroat. Chem.* **2006**, *17*(1), 57–60.

* To whom correspondence should be addressed. Phone: +90-312-2126720. Fax: +90-312-2232395. E-mail: zkilic@science.ankara.edu.tr.

glycols,⁴ have been shown to yield spiro-, ansa-, binoarchitectures or the mixtures of these compounds. In recent years, two interesting papers about the reactions of bifunctional reagents with fluoro- and chlorophosphazenes have appeared in the literature, and it has been reported that, in these reactions, ansa-, spiro-, ansa-spiro-, and bis(ansa-substituted)-cyclophosphazenes have been isolated.⁵ Our group has recently synthesized four novel families of partially substituted phosphazene derivatives with N₂O_x (x=2,3) donor-type crown ethers,⁶ bulky difunctional aminopodands,⁷ and tetrafunctional aminopodands,⁸ namely, spiro-crypta, spiro-crown (PNP-lariat), spiro-ansa-spiro-, and spiro-bino-spiro-phosphazenes. Another area of interest is the ring-opening polymerization leading to the preparation of different polyphosphazene types, cycloliner or cyclomatrix polymers.⁹ The use of cyclophosphazenes as ligands, in particular, for transition metal ions is also an area of interest.¹⁰ Coordination through a ring nitrogen atom or a substituted ligating group

to the phosphazene ring can result in interesting structures.¹¹ The investigation of the stereogenic properties of cyclophosphazene derivatives has been a new subject of interest for the last five years.^{2e,3a,12} Cyclophosphazene derivatives have given rise to considerable interest for the further design of highly selective anticancer¹³ and antibacterial¹⁴ reagents. Aziridine-crown-substituted phosphazene synthesized by Brandt et al. cleaves DNA and halts the growth of cancer cells.¹⁵ In addition, cyclophosphazenes have found industrial applications in the production of inflammable textile fibers, advanced elastomers,¹⁶ rechargeable lithium batteries,¹⁷ and biomedical materials including synthetic bones.¹⁸

We report here (i) the synthesis of spiro-bino-spiro- (**19**) and spiro-crypta (**21**, **22**, and **25**) phosphazenes from the reactions of N₃P₃Cl₆ with the aminopodand (**4**) and dibenzodiazacrown ethers (**5**, **6**, and **9**), respectively; (ii) the substitution of the Cl atoms of spiro-ansa-spiro (**11**) by pyrrolidine and DASD giving the respective fully substituted phosphazenes (**14** and **16**); (iii) the substitution of the Cl atoms of spiro-crypta phosphazenes (**23** and **24**) by pyrrolidine leading to the geminal pyrrolidine-substituted phosphazenes (**26** and **27**) (Scheme 1); (iv) the analytical, physical and spectral (IR, ¹H, ¹³C, and ³¹P NMR, HETCOR, and MS) data of **10**, **14**, **16**, **19**, **21**, **22**, and **25–27** in comparison to the related compounds (**11–13**, **15**, **17**, **18**, **20^{8a}** and **23**, **24**)^{6a}; (v) the X-ray structural analyses of **16** and **22**; and (vi) the relationship between the δP shifts and the X-ray crystallographic data.

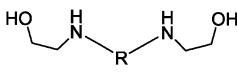
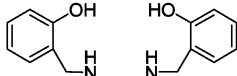
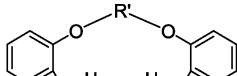
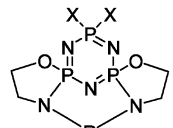
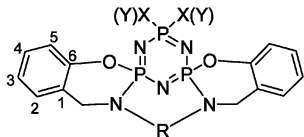
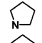
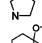
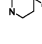
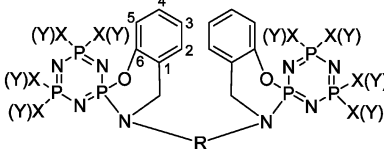
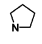
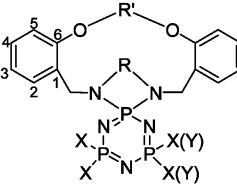
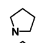
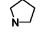
Experimental Section

General Methods. All reactions were performed under an inert atmosphere of argon. The reaction solvents were dried and distilled by standard methods before use. Compound **1** was obtained from Aldrich Chemical Co. and used without further purification. Melting points were measured on a Gallenkamp apparatus using a capillary tube. ¹H, ¹³C, and ³¹P NMR and HETCOR spectra were obtained on a Bruker DPX FT-NMR (400 MHz) spectrometer (SiMe₄, as an internal standard and 85% H₃PO₄ as an external standard). IR spectra were recorded on a Mattson 1000 FTIR spectrometer in KBr disks and were reported in per centimeter units. Microanalyses were carried out by the microanalytical service of TUBITAK (Turkey). Electrospray-ionization (ESI) and electron-impact (EI)

- (2) (a) Kılıç, A.; Kılıç, Z.; Shaw, R. A. *Phosphorus Sulfur Silicon Relat. Elem.* **1991**, *57*, 111–117. (b) Labarre, J. F.; Guersch, G.; Sourmies, F.; Lahana, R.; Enjalbert, R.; Galy, J. *J. Mol. Struct.* **1984**, *116*, 75–88. (c) Labarre, J. F. *Top. Curr. Chem.* **1985**, *129*, 173–230. (d) Wilson, M.; Lafaille, L.; Vidaud, L.; Labarre, J. E. *Phosphorus Sulfur Relat. Elem.* **1987**, *29*, 147–157. (e) Coles, S. J.; Davies, D. B.; Eaton, R. J.; Hursthouse, M. B.; Kılıç, A.; Mayer, T. A.; Shaw, R. A.; Yenilmez, G. *J. Chem. Soc., Dalton Trans.* **2002**, 365–370.
- (3) (a) Bešli, S.; Coles, S. J.; Davies, D. B.; Eaton, R. J.; Hursthouse, M. B.; Kılıç, A.; Shaw, R. A.; Çiftçi, G. Y.; Yeşilot, S. *J. Am. Chem. Soc.* **2003**, *125*, 4943–4950. (b) Parwolik-Czomperlic, I.; Brandt, K.; Clayton, T. A.; Davies, D. B.; Eaton, R. J.; Shaw, R. A. *Inorg. Chem.* **2002**, *41*, 4944–4951. (c) Yıldız, M.; Kılıç, Z.; Hökelek, T. *J. Mol. Struct.* **1999**, *510*, 227–235. (d) Kılıç, A.; Begeç, S.; Çetinkaya, B.; Kılıç, Z.; Hökelek, T.; Gündüz, N.; Yıldız, M. *Heteroat. Chem.* **1996**, *7*(4), 249–256. (e) Allcock, H. R.; Sunderland, N. J.; Primrose, A. P.; Rheingold, A. L.; Guzei, I. A.; Parvez, M. *Chem. Mater.* **1999**, *11*, 2478–2485. (f) Carriedo, G. A.; Martinez, J. I. F.; Alonso, F. J. G.; Gonzalez, E. R.; Soto, A. P. *Eur. J. Inorg. Chem.* **2002**, 1502–1510. (g) Chandrasekhar, V.; Athimoolam, A.; Srivatsan, S. G.; Sundaram, P. S.; Verma, S.; Steiner, A.; Zacchini, S.; Butcher, R. *Inorg. Chem.* **2002**, *41*, 5162–5173. (h) Allcock, H. R.; Dembek, A.; Mang, M. N.; Riding, G. H.; Parvez, M. *Inorg. Chem.* **1992**, *31*, 2734–2739. (i) Reuben, J. *J. Magn. Reson. Chem.* **1987**, *25*, 1049–1053. (j) Karthikeyan, S.; Krishnamurty, S. S. *Z. Anorg. Allg. Chem.* **1984**, *513*, 231–240. (k) Allcock, H. R.; Ngo, D. C.; Parvez, M.; Whittle, R. R.; Bird-sall, W. J. *J. Am. Chem. Soc.* **1991**, *113*, 2628–2634. (l) Harris, P. J.; Williams, K. B. *Inorg. Chem.* **1984**, *23*, 1496–1498.
- (4) (a) Shaw, R. A.; Ture, S. *Phosphorus Sulfur Silicon Relat. Elem.* **1991**, *57*, 103–109. (b) Al-Madfa, H. A.; Shaw, R. A.; Ture, S. *Phosphorus Sulfur Silicon Relat. Elem.* **1990**, *53*, 333–338.
- (5) (a) Chandrasekhar, V.; Nagendran, S. *Chem. Soc. Rev.* **2001**, *30*, 193–203. (b) Chandrasekhar, V.; Krishnan, V. *Adv. Inorg. Chem.* **2002**, *53*, 159–211.
- (6) (a) Bilge, S.; Kılıç, Z.; Çaylak, N.; Hökelek, T. *J. Mol. Struct.* **2004**, *707*, 139–146. (b) Tercan, B.; Hökelek, T.; Bilge, S.; Demiriz, Ş.; Kılıç, Z. *Acta Crystallogr.* **2004**, *E60*, 1369–1372.
- (7) (a) Çaylak, N.; Hökelek, T.; Bilge, S.; Özgüç, B.; Kılıç, Z. *Acta Crystallogr.* **2004**, *C60*, 461–463. (b) Tercan, B.; Hökelek, T.; Bilge, Ş.; Özgüç, B.; Kılıç, Z. *Acta Crystallogr.* **2004**, *C60*, 381–383. (c) Özgüç, B.; Bilge, S.; Çaylak, N.; Demiriz, Ş.; İşler, H.; Hayvalı, M.; Kılıç, Z.; Hökelek, T. *J. Mol. Struct.* **2005**, *748*, 39–47.
- (8) (a) Bilge, S.; Natsagdorj, A.; Demiriz, Ş.; Çaylak, N.; Kılıç, Z.; Hökelek, T. *Helv. Chim. Acta* **2004**, *87*, 2088–2099. (b) Safran, S.; Hökelek, T.; Bilge, S.; Demiriz, Ş.; Natsagdorj, A.; Kılıç, Z. *Anal. Sci.* **2005**, *21*, 77–78. (c) Tercan, B.; Hökelek, T.; Bilge, S.; Natsagdorj, A.; Demiriz, Ş.; Kılıç, Z. *Acta Crystallogr.* **2004**, *E60*, 795–797.
- (9) (a) Dez, I.; Levalois-Mitjaville, J.; Grützmacher, H.; Gramlinch, V.; Jaeger, R. *Eur. J. Inorg. Chem.* **1999**, 1673–1684. (b) Mathew, D.; Nair, C. P. R.; Ninan, K. N. *Polym. Int.* **2000**, *49*, 48–56.
- (10) Chandrasekhar, V.; Vivekanandan, K.; Nagendran, S.; Senthil Andavan, G. T.; Weathers, N. R.; Yarbrough, J. C.; Cordes, A. W. *Inorg. Chem.* **1998**, *37*, 6192–6198.

- (11) (a) Chandrasekhar, V.; Thomas, K. R. *J. Appl. Organomet. Chem.* **1993**, *7*, 1–31. (b) Allcock, H. R.; Turner, M. N. *Macromolecules* **1993**, *26*, 3–10.
- (12) (a) Uslu, A.; Coles, S. J.; Davies, D. B.; Eaton, R. J.; Hursthouse, M. B.; Kılıç, A.; Shaw, R. A. *Eur. J. Inorg. Chem.* **2005**, 1042–1047. (b) Bešli, S.; Coles, S. J.; Davies, D. B.; Eaton, R. J.; Hursthouse, M. B.; Kılıç, A.; Shaw, R. A.; Uslu, A.; Yeşilot, S. *Inorg. Chem. Commun.* **2004**, *7*, 842–846.
- (13) (a) Labarre, J. F.; Bovin, O. J.; Galy, J. *Acta Crystallogr.* **1979**, *B35*, 1182–1186. (b) Baek, H.; Cho, Y.; Lee, C.; Shon, Y. *Anti-Cancer Drugs* **2000**, *11*, 715–725.
- (14) Konar, V.; Yılmaz, Ö.; Öztürk, A. I.; Kirbağ, S.; Arslan, M. *Bioorg. Chem.* **2000**, *28*, 214–225.
- (15) Brandt, K.; Bartczak, T. J.; Kruszynski, R.; Parwolik-Czomperlic, I. *Inorg. Chim. Acta* **2001**, *322*, 138–144.
- (16) Allcock, H. R.; Napierala, M. E.; Cameron, C. G.; O'Connor, S. J. M. *Macromolecules* **1996**, *29*, 1951–1956.
- (17) (a) Allcock, H. R.; Kwon, S. *Macromolecules* **1986**, *19*, 1502–1508. (b) Xu, G.; Lu, Q.; Yu, B.; Wen, L. *Solid State Ionics* **2006**, *177*, 305–309.
- (18) Greish, Y. E.; Bender, J. D.; Lakshmi, S.; Brown, P. W.; Allcock, H. R.; Laurencin, C. T. *Biomaterials* **2005**, *26* (1), 1–9.

Scheme 1

	R	R'	X	Y	No
 Aminopodand	CH ₂ -CH ₂	-	-	-	1
 Aminopodand	CH ₂ -CH ₂	-	-	-	2
	CH ₂ -CH ₂ -CH ₂	-	-	-	3
	CH ₂ -CH ₂ -CH ₂ -CH ₂	-	-	-	4
 Dibenzo-diaza-crown ether	CH ₂ -CH ₂	CH ₂ -CH ₂	-	-	5
	CH ₂ -CH ₂ -CH ₂	CH ₂ -CH ₂	-	-	6
	CH ₂ -CH ₂	(CH ₂ -CH ₂) ₂ O	-	-	7
	CH ₂ -CH ₂ -CH ₂	(CH ₂ -CH ₂) ₂ O	-	-	8
	CH ₂ -CH ₂ -CH ₂ -CH ₂	(CH ₂ -CH ₂) ₂ O	-	-	9
 spiro-ansa-spiro-Phosphazene	CH ₂ -CH ₂	-	Cl	-	10
 spiro-ansa-spiro-Phosphazene	CH ₂ -CH ₂	-	Cl	-	11
	CH ₂ -CH ₂ -CH ₂	-	Cl	-	12
	CH ₂ -CH ₂ -CH ₂ -CH ₂	-	Cl	-	13
	CH ₂ -CH ₂	-	-		14
	CH ₂ -CH ₂ -CH ₂	-	-		15
	CH ₂ -CH ₂	-	-		16
 spiro-bino-spiro-Phosphazene	CH ₂ -CH ₂	-	Cl	-	17
	CH ₂ -CH ₂ -CH ₂	-	Cl	-	18
	CH ₂ -CH ₂ -CH ₂ -CH ₂	-	Cl	-	19
	CH ₂ -CH ₂ -CH ₂	-	-		20
 spiro-Crypta phosphazene	CH ₂ -CH ₂	CH ₂ -CH ₂	Cl	-	21
	CH ₂ -CH ₂ -CH ₂	CH ₂ -CH ₂	Cl	-	22
	CH ₂ -CH ₂	(CH ₂ -CH ₂) ₂ O	Cl	-	23
	CH ₂ -CH ₂ -CH ₂	(CH ₂ -CH ₂) ₂ O	Cl	-	24
	CH ₂ -CH ₂ -CH ₂ -CH ₂	(CH ₂ -CH ₂) ₂ O	Cl	-	25
	CH ₂ -CH ₂	(CH ₂ -CH ₂) ₂ O	Cl		26
	CH ₂ -CH ₂ -CH ₂	(CH ₂ -CH ₂) ₂ O	Cl		27

mass spectrometric analysis were performed on the AGILEND 1100 MSD and VG-ZAPSPEC spectrometers, respectively. Thin-layer chromatography (TLC) was performed on Merck DC Alufolien Kiesegel 60 B₂₅₄ sheets. Column chromatography was performed on Merck Kiesegel 60 (230–400 mesh ATSM) silica gel.

Preparation of Compounds. Phosphazene derivatives **11–13**, **15**, **17**, **18**, **20**^{8a} **23**, and **24**^{6a} were prepared according to the published procedures.

The preparation and crystallographic data of 8,8-dichloro-1,2,10,11,13,14-hexahydro-6 λ^5 ,8 λ^5 ,10 λ^5 -6,10-nitrilo[1,3,5,7,2,4,6]-tetrazatriphosphonino-bis[1,3,2]oxazaphosphorine (**10**) were published before.^{8b} The MS, IR, and ¹H, ¹³C, and ³¹P NMR data of **10** will be discussed in this paper. ESI-MS (fragments based on ³⁵Cl, I_r, %): *m/z* 348 ([*M* + H]⁺, 29), 314 ([(*M* - Cl)]⁺, 7), 291 ([(*M* - C₂H₄ON)]⁺, 24). IR (KBr, cm⁻¹): ν 2977–2857 (C–H aliph), 1188

(P=N), 587 (P–Cl). ¹H NMR (400 MHz, CDCl₃): δ 3.35 (m, 4H, N–CH₂), 3.45 (m, 4H, O–CH₂–CH₂), 4.48 (m, 4H, O–CH₂). ¹³C NMR (400 MHz, CDCl₃): δ 45.0 (triplet, ²J_{PC} = 7.8 Hz, N–CH₂), 48.7 (triplet, ²J_{PC} = 11.2 Hz, O–CH₂–CH₂), 67.0 (O–CH₂).

18,19-Dihydro-8,8-dipyrrolidino-1-yl-6 λ^5 ,8 λ^5 ,10 λ^5 -6,10-nitrilo-16H,21H[1,3,5,7,2,4,6]tetrazatriphosphonino[2,1-b:6,7-b']bis-[1,3,2]benzoxazaphosphorine (14). A solution of 0.50 mL (6.05 mmol) of pyrrolidine in 50 mL of dry THF was slowly added to a stirred solution of 0.50 g (1.06 mmol) of **11** in 100 mL of dry THF at room temperature. The solution was heated to reflux for 48 h with argon being passed over the mixture. The precipitated amine hydrochloride was filtered off, and the solvent was evaporated. The residue was subjected to column chromatography [benzene/THF (1/1), *R_f* = 0.84] and crystallized from CH₃CN. Yield: 0.42 g (74%). mp: 250 °C. Anal. Calcd for C₂₄H₃₂N₇O₂P₃: C, 53.04; H,

5.93; N, 18.04. Found: C, 53.44; H, 5.92; N, 17.95. ESI-MS (I_r , %): m/z 530 ($[(M - \text{CH}_2) + \text{H}]^+$, 60), 516 ($[(M - \text{C}_2\text{H}_4) + \text{H}]^+$, 78). IR (KBr, cm^{-1}): ν 3059, 3040 (C–H arom), 2965–2828 (C–H aliph), 1583 (C=C), 1182 (P=N). ^1H NMR (400 MHz, CDCl_3): δ 1.86 (m, 8H, N–CH₂–CH₂), 3.12 (m, 2H, *ansa* N–CH₂), 3.25 (m, 8H, pyrrolidine N–CH₂), 3.43 (m, 2H, *ansa* N–CH₂), 3.84 (q, 2H, $^3J_{\text{PH}} = 15.0$ Hz, Ar–CH₂–N), 4.47 (q, 2H, $^3J_{\text{PH}} = 15.0$ Hz, Ar–CH₂–N), 6.96–7.20 (8H, Ar–H). ^{13}C NMR (400 MHz, CDCl_3 , numberings of aromatic carbons are given in Scheme 1): δ 26.32 ($^3J_{\text{PC}} = 9.3$ Hz, N–CH₂–CH₂), 26.37 ($^3J_{\text{PC}} = 9.0$ Hz, N–CH₂–CH₂), 46.1 ($^2J_{\text{PC}} = 3.8$ Hz, pyrrolidine N–CH₂), 46.3 ($^2J_{\text{PC}} = 4.0$ Hz, pyrrolidine N–CH₂), 51.6 (Ar–CH₂–N), 53.6 (*ansa* N–CH₂), 119.0 (triplet, $^3J_{\text{PC}} = 8.6$ Hz, C₅), 123.0 (C₃), 124.8 (triplet, $^3J_{\text{PC}} = 8.1$ Hz, C₁), 126.4 (C₄), 128.4 (C₂), 151.2 (triplet, $^2J_{\text{PC}} = 6.1$ Hz, C₆).

18,19-Dihydro-8,8-bis(1,4-dioxo-8-azaspiro[4,5]decane)-1-yl-6 λ^5 ,8 λ^5 ,10 λ^5 -6,10-nitrilo-16H,21H-[1,3,5,7,2,4,6]tetrazatriphosphonino[2,1-b:6,7-b']bis[1,3,2]benzoxazaphosphorine (16). A solution of 0.80 mL (6.24 mmol) of DASD in 50 mL of dry THF was slowly added to a stirred solution of 0.50 g (1.06 mmol) of **11** in 100 mL of dry THF at room temperature. The solution was heated to reflux for 40 h with argon being passed over the mixture. The precipitated amine hydrochloride was filtered off, and the solvent was evaporated. The residue was subjected to column chromatography [benzene/THF (1/1), $R_f = 0.37$] and crystallized from *n*-heptane. Yield: 0.49 g (68%). mp: 252 °C. Anal. Calcd for C₃₀H₄₀N₇O₆P₃: C, 52.40; H, 5.86; N, 14.26. Found: C, 52.81; H, 5.90; N, 14.08. CI-MS (I_r , %): m/z 688 ($[M + \text{H}]^+$, 100), 545 ($[M - \text{DASD}]^+$, 29). IR (KBr, cm^{-1}): ν 3061, 3030 (C–H arom), 2982–2836 (C–H aliph.), 1585 (C=C), 1180 (P=N). ^1H NMR (400 MHz, CDCl_3): δ 1.62 (br, 2H, N–CH₂–CH₂), 1.77 (br, 6H, N–CH₂–CH₂), 3.15 (br, 2H, *ansa* N–CH₂), 3.32 (br, 4H, DASD N–CH₂), 3.38 (br, 4H, DASD N–CH₂), 3.44 (br, 2H, *ansa* N–CH₂), 3.84 (q, 2H, $^3J_{\text{PH}} = 14.8$ Hz, Ar–CH₂–N), 3.99 (s, 4H, O–CH₂), 4.00 (s, 4H, O–CH₂), 4.48 (q, 2H, $^3J_{\text{PH}} = 14.8$ Hz, Ar–CH₂–N), 6.99–7.32 (8H, Ar–H). ^{13}C NMR (400 MHz, CDCl_3): δ 35.3 ($^3J_{\text{PC}} = 4.9$ Hz, N–CH₂–CH₂), 35.6 ($^3J_{\text{PC}} = 5.7$ Hz, N–CH₂–CH₂), 42.6 (DASD N–CH₂), 42.8 (DASD N–CH₂), 43.6 (*ansa* N–CH₂), 51.6 (Ar–CH₂–N), 64.2 (O–CH₂), 64.3 (O–CH₂), 107.6 (O–C–O), 119.1 (C₅), 123.2 (C₃), 124.6 (C₁), 126.4 (C₄), 128.5 (C₂), 151.1 (C₆).

3,3'-Butane-1,4-diylbis[4',4',6',6'-tetrachloro-3,4-dihydrospiro[1,3,2-benzoxazaphosphorine-2,2' λ^5 -[4 λ^5 ,6 λ^5][1,3,5,2,4,6]triazatriphosphorine]] (19). K₂CO₃ (2.80 g, 20.0 mmol) was added to a stirred solution of 3.00 g (10.0 mmol) of **4** in 200 mL of dry THF. The mixture was refluxed for 2 h and then cooled. A solution of 1.70 g (5.00 mmol) of N₃P₃Cl₆ in 100 mL of dry THF was added dropwise to the stirred mixture at –10 °C for over 1 h. After the mixture had been allowed to warm to ambient temperature, it was stirred for 30 h with Ar being passed over the reaction mixture. The precipitated amine hydrochloride and excess of K₂CO₃ were filtered off, and the solvent was evaporated. The residue was subjected to column chromatography with benzene. The first eluted compound is **19** (benzene, $R_f = 0.62$), and it was crystallized from benzene. Yield: 1.11 g (52%). mp: 110 °C. Anal. Calcd for C₁₈H₂₀Cl₈N₈O₂P₆: C, 25.44; H, 2.37; N, 13.19. Found: C, 25.64; H, 2.39; N, 13.16. CI-MS (fragments based on ^{35}Cl , I_r , %): m/z 847 ($[M + \text{H}]^+$, 45), 776 ($[M - 2\text{Cl}]^+$, 2). IR (KBr, cm^{-1}): ν 3069, 3031 (C–H arom), 2934–2847 (C–H aliph), 1587 (C=C), 1173 (P=N), 597 (P–Cl). ^1H NMR (400 MHz, CDCl_3): δ 1.72 (t, 4H, $^3J_{\text{HH}} = 5.9$ Hz, N–CH₂–CH₂), 3.12 (m, 4H, $^3J_{\text{PH}} = 11.8$ Hz, $^3J_{\text{HH}} = 5.9$ Hz, N–CH₂), 4.24 (d, 4H, $^3J_{\text{PH}} = 15.7$ Hz, Ar–CH₂–N), 7.06–7.39 (8H, Ar–H). ^{13}C NMR (400 MHz, CDCl_3): δ 24.7 ($^3J_{\text{PC}} =$

4.2 Hz, N–CH₂–CH₂), 47.3 ($^2J_{\text{PC}} = 3.7$ Hz, N–CH₂), 47.9 (Ar–CH₂–N), 118.7 ($^3J_{\text{PC}} = 8.3$ Hz, C₅), 123.7 ($^3J_{\text{PC}} = 7.3$ Hz, C₁), 124.3 (C₃), 126.6 (C₄), 129.1 (C₂), 149.9 ($^2J_{\text{PC}} = 8.5$ Hz, C₆). The second product is **13**.^{8a}

7,10-(Ethane-1,2-diylidiodioxydi-o-phenylene-dimethylene)-4,4,6,6-tetrachloro-2 λ^5 ,4 λ^5 ,6 λ^5 -triphosphaza(6-P^V)-1,3,5,7,10-pentaazaspiro[4.5]undeca-1,3,5-triene (21). A solution of 1.15 g (3.30 mmol) of N₃P₃Cl₆ in 100 mL of dry THF was slowly added to a solution of 1.00 g (3.36 mmol) of **5** and 1.90 mL (13.6 mmol) of triethylamine in 50 mL of dry THF. The mixture was refluxed for 8 h with argon being passed over the reaction mixture and then cooled. The precipitated amine hydrochloride was filtered off, and the solvent was evaporated under reduced pressure. The residue was subjected to column chromatography (benzene, $R_f = 0.56$) and crystallized from a CH₂Cl₂/*n*-heptane (1/1) mixture. Yield: 1.14 g (60%). mp: 238 °C. Anal. Calcd for C₁₈H₂₀Cl₄N₅O₂P₃: C, 37.72; H, 3.52; N, 12.22. Found: C, 38.05; H, 3.55; N, 12.31. CI-MS (fragments based on ^{35}Cl , I_r , %): m/z 572 ($[M + \text{H}]^+$, 77). IR (KBr, cm^{-1}): ν 3063, 3038 (C–H arom), 2940–2878 (C–H aliph), 1599 (C=C), 1233, 1173 (P=N), 568 (P–Cl). ^1H NMR (400 MHz, CDCl_3): δ 2.95 (m, 2H, $^3J_{\text{PH}} = 10.4$ Hz, $^2J_{\text{HH}} = 5.7$ Hz, N–CH₂), 3.03 (m, 2H, $^3J_{\text{PH}} = 10.4$ Hz, $^2J_{\text{HH}} = 5.7$ Hz, N–CH₂), 3.95 (q, 2H, $^3J_{\text{PH}} = 13.8$ Hz, $^2J_{\text{HH}} = 9.1$ Hz, Ar–CH₂–N), 4.45 (m, 4H, Ar–O–CH₂), 4.67 (q, 2H, $^3J_{\text{PH}} = 13.8$ Hz, $^2J_{\text{HH}} = 9.1$ Hz, Ar–CH₂–N), 6.89–7.29 (8H, Ar–H). ^{13}C NMR (400 MHz, CDCl_3): δ 44.5 ($^2J_{\text{PC}} = 17.8$ Hz, N–CH₂), 46.7 ($^2J_{\text{PC}} = 7.2$ Hz, Ar–CH₂–N), 65.8 (Ar–O–CH₂), 111.3 (C₅), 120.6 (C₃), 124.6 ($^3J_{\text{PC}} = 3.1$ Hz, C₁), 129.4 (C₄), 131.6 (C₂), 157.6 (C₆).

7,11-(Ethane-1,2-diylidiodioxydi-o-phenylene-dimethylene)-4,4,6,6-tetrachloro-2 λ^5 ,4 λ^5 ,6 λ^5 -triphosphaza(6-P^V)-1,3,5,7,11-pentaazaspiro[5.5]dodeca-1,3,5-triene (22). Compound **22** was obtained as described for **21** with 1.00 g (3.21 mmol) of **6**, 1.80 mL (12.9 mmol) of triethylamine, and 1.08 g (3.10 mmol) of N₃P₃Cl₆ (6 h) (benzene, $R_f = 0.72$), and it was crystallized from *n*-heptane. Yield: 1.24 g (68%). mp: 247 °C. Anal. Calcd for C₁₉H₂₂Cl₄N₅O₂P₃: C, 38.87; H, 3.78; N, 11.93. Found: C, 38.42; H, 3.75; N, 11.96. CI-MS (fragments based on ^{35}Cl , I_r , %): m/z 586 ($[M + \text{H}]^+$, 98). IR (KBr, cm^{-1}): ν 3067, 3025 (C–H arom), 2967–2840 (C–H aliph), 1601 (C=C), 1238, 1182 (P=N), 573 (P–Cl). ^1H NMR (400 MHz, CDCl_3): δ 1.58 (m, 2H, N–CH₂–CH₂), 2.97 (m, 2H, $^3J_{\text{PH}} = 12.8$ Hz, $^3J_{\text{HH}} = 9.8$ Hz, N–CH₂), 3.35 (m, 2H, $^3J_{\text{PH}} = 12.8$ Hz, $^3J_{\text{HH}} = 9.8$ Hz, N–CH₂), 3.66 (q, 2H, $^3J_{\text{PH}} = 13.1$ Hz, $^2J_{\text{HH}} = 7.2$ Hz, Ar–CH₂–N), 4.37 (m, 2H, Ar–O–CH₂), 4.49 (m, 2H, Ar–O–CH₂), 4.57 (q, 2H, $^3J_{\text{PH}} = 13.1$ Hz, $^2J_{\text{HH}} = 7.2$ Hz, Ar–CH₂–N), 6.85–7.23 (8H, Ar–H). ^{13}C NMR (400 MHz, CDCl_3): δ 23.8 ($^3J_{\text{PC}} = 4.7$ Hz, N–CH₂–CH₂), 46.7 (N–CH₂), 48.1 (Ar–CH₂–N), 65.8 (Ar–O–CH₂), 111.7 (C₅), 120.2 (C₃), 126.8 ($^3J_{\text{PC}} = 6.2$ Hz, C₁), 129.0 (C₄), 131.9 (C₂), 157.2 (C₆).

7,12-(Pentane-3-oxa-1,5-diylidiodioxydi-o-phenylene-dimethylene)-4,4,6,6-tetrachloro-2 λ^5 ,4 λ^5 ,6 λ^5 -triphosphaza(6-P^V)-1,3,5,7,12-pentaazaspiro[6.5]trideca-1,3,5-triene (25). Compound **25** was prepared as described for **21** with 1.00 g (2.70 mmol) of **9**, 1.50 mL (10.8 mmol) of triethylamine, and 0.92 g (2.65 mmol) of N₃P₃Cl₆ (8 h) (benzene, $R_f = 0.50$), and it was crystallized from a CH₂Cl₂/*n*-heptane (1/1) mixture. Yield: 1.20 g (70%). mp: 212 °C. Anal. Calcd for C₂₂H₂₈Cl₄N₅O₃P₃: C, 40.95; H, 4.37; N, 10.85. Found: C, 42.16; H, 4.40; N, 10.93. CI-MS (fragments based on ^{35}Cl , I_r , %): m/z 644 ($[M + \text{H}]^+$, 81). IR (KBr, cm^{-1}): ν 3065, 3028 (C–H arom), 2934–2846 (C–H aliph), 1601 (C=C), 1229, 1163 (P=N), 570 (P–Cl). ^1H NMR (400 MHz, CDCl_3): δ 0.91 (t, 2H, $^3J_{\text{HH}} = 6.7$ Hz, N–CH₂–CH₂), 1.33 (m, 2H, $^3J_{\text{HH}} = 6.7$ Hz, N–CH₂–CH₂), 3.38 (q, 2H, $^3J_{\text{PH}} = 15.6$ Hz, N–CH₂), 3.44 (q,

2H, $^3J_{\text{PH}} = 15.6$ Hz, N–CH₂), 3.68 (q, 2H, $^3J_{\text{PH}} = 13.6$ Hz, $^2J_{\text{HH}} = 7.3$ Hz, Ar–CH₂–N), 3.69 (m, 2H, $^2J_{\text{HH}} = 18.9$ Hz, $^3J_{\text{HH}} = 8.6$ Hz, $^3J_{\text{HH}} = 9.5$ Hz, Ar–O–CH₂–CH₂), 4.08 (t, 2H, $^2J_{\text{HH}} = 18.9$ Hz, $^3J_{\text{HH}} = 8.6$ Hz, $^3J_{\text{HH}} = 9.5$ Hz, Ar–O–CH₂–CH₂), 4.70 (q, 2H, $^3J_{\text{PH}} = 13.6$ Hz, $^2J_{\text{HH}} = 7.3$ Hz, Ar–CH₂–N), 4.26 (q, 2H, $^2J_{\text{HH}} = 11.4$ Hz, $^3J_{\text{HH}} = 8.6$ Hz, $^3J_{\text{HH}} = 9.5$ Hz, Ar–O–CH₂), 4.35 (t, 2H, $^2J_{\text{HH}} = 11.4$ Hz, $^3J_{\text{HH}} = 8.6$ Hz, $^3J_{\text{HH}} = 9.5$ Hz, Ar–O–CH₂), 6.84–7.29 (8H, Ar–H). ¹³C NMR (400 MHz, CDCl₃): δ 27.9 (N–CH₂–CH₂), 48.2 ($^2J_{\text{PC}} = 7.0$ Hz, N–CH₂), 50.3 ($^2J_{\text{PC}} = 7.7$ Hz, Ar–CH₂–N), 66.8 (Ar–O–CH₂), 69.8 (Ar–O–CH₂–CH₂), 110.6 (C₅), 120.2 (C₃), 127.0 ($^3J_{\text{PC}} = 5.7$ Hz, C₁), 129.0 (C₄), 131.7 (C₂), 157.3 (C₆).

7,10-(Pentane-3-oxa-1,5-diylidioxidi-o-phenylene-dimethylene)-6,6-dichloro-4,4-bis(pyrrolidine-1-yl)-2 λ^5 ,4 λ^5 ,6 λ^5 -triphosphaza-(6-P^V)-1,3,5,7,10-pentaazaspiro[4.5]undeca-1,3,5-triene (26). A solution of 0.80 mL (9.73 mmol) of pyrrolidine in 50 mL of dry THF was slowly added to a stirred solution of 0.50 g (0.81 mmol) of **23** in 100 mL of dry THF at room temperature. The solution was heated to reflux for 42 h with argon being passed over the mixture. The precipitated amine hydrochloride was filtered off, and the solvent was evaporated. The residue was subjected to column chromatography [benzene/THF (1/1), $R_f = 0.90$] and crystallized from CH₃CN. Yield: 0.34 g (61%). mp: 223 °C. Anal. Calcd for C₂₈H₄₀Cl₂N₇O₃P₃: C, 48.99; H, 5.87; N, 14.28. Found: C, 49.00; H, 5.90; N, 14.16. ESI-MS (fragments based on ³⁵Cl, I_r , %): m/z 686 ([M + H]⁺, 100). IR (KBr, cm⁻¹): ν 3065, 3040 (C–H arom), 2913–2826 (C–H aliph), 1234 (P=N), 1603 (C=C), 579 (P–Cl). ¹H NMR (400 MHz, CDCl₃): δ 1.95 (m, 8H, N–CH₂–CH₂), 2.75 (m, 2H, *spiro* N–CH₂), 3.04 (m, 2H, $^2J_{\text{HH}} = 12.3$ Hz, $^3J_{\text{HH}} = 9.4$ Hz, $^3J_{\text{HH}} = 9.3$ Hz, Ar–O–CH₂), 3.32 (m, 2H, *spiro* N–CH₂), 3.45 (m, 8H, *pyrrolidine* N–CH₂), 3.77 (q, 2H, $^3J_{\text{PH}} = 12.2$ Hz, $^2J_{\text{HH}} = 9.1$ Hz, Ar–CH₂–N), 3.85 (m, 2H, $^2J_{\text{HH}} = 12.3$ Hz, $^3J_{\text{HH}} = 9.4$ Hz, $^3J_{\text{HH}} = 9.3$ Hz, Ar–O–CH₂–CH₂), 4.24 (m, 2H, $^2J_{\text{HH}} = 12.3$ Hz, $^3J_{\text{HH}} = 9.4$ Hz, $^3J_{\text{HH}} = 9.3$ Hz, Ar–O–CH₂–CH₂), 4.28 (m, 2H, $^2J_{\text{HH}} = 12.3$ Hz, $^3J_{\text{HH}} = 9.4$ Hz, $^3J_{\text{HH}} = 9.3$ Hz, Ar–O–CH₂), 4.52 (q, 2H, $^3J_{\text{PH}} = 12.2$ Hz, $^2J_{\text{HH}} = 9.1$ Hz, Ar–CH₂–N), 6.80–7.30 (8H, Ar–H). ¹³C NMR (400 MHz, CDCl₃): δ 23.8 ($^3J_{\text{PC}} = 9.2$ Hz, N–CH₂–CH₂), 42.2 ($^2J_{\text{PC}} = 17.3$ Hz, *spiro* N–CH₂), 44.5 ($^2J_{\text{PC}} = 6.9$ Hz, Ar–CH₂–N), 46.7 ($^2J_{\text{PC}} = 4.9$ Hz, *pyrrolidine* N–CH₂), 67.5 (Ar–O–CH₂), 69.4 (Ar–O–CH₂–CH₂), 110.2 (C₅), 120.0 (C₃), 122.6 (C₁), 129.8 (C₄), 131.9 (C₂), 158.0 (C₆).

7,11-(Pentane-3-oxa-1,5-diylidioxidi-o-phenylene-dimethylene)-6,6-dichloro-4,4-bis(pyrrolidine-1-yl)-2 λ^5 ,4 λ^5 ,6 λ^5 -triphosphaza-(6-P^V)-1,3,5,7,11-pentaazaspiro[5.5]dodeca-1,3,5-triene (27). Compound **27** was prepared As described for **26** with 0.50 g (0.79 mmol) of **24** and 0.80 mL (9.67 mmol) of pyrrolidine (36 h) [benzene/THF (1/1) mixture, $R_f = 0.82$], and it was crystallized from CH₃CN. Yield: 0.31 g (55%). mp: 191 °C. Anal. Calcd for C₂₉H₄₂Cl₂N₇O₃P₃: C, 49.72; H, 6.04; N, 14.00. Found: C, 50.01; H, 5.99; N, 13.92. ESI-MS (fragments based on ³⁵Cl, I_r , %): m/z 700 ([M + H]⁺, 45). IR (KBr, cm⁻¹): ν 3063, 3041 (C–H arom), 2922–2849 (C–H aliph), 1603 (C=C), 1229 (P=N), 577 (P–Cl). ¹H NMR (400 MHz, CDCl₃): δ 1.28 (m, 2H, *spiro* N–CH₂–CH₂), 1.73 (m, 8H, *pyrrolidine* N–CH₂–CH₂), 2.79 (m, 2H, $^3J_{\text{PH}} = 15.6$ Hz, *spiro* N–CH₂), 3.10 (m, 2H, $^3J_{\text{PH}} = 15.6$ Hz, *spiro* N–CH₂), 3.20 (m, 8H, $^3J_{\text{PH}} = 4.2$ Hz, *pyrrolidine* N–CH₂), 3.38 (q, 2H, $^3J_{\text{PH}} = 12.7$ Hz, $^2J_{\text{HH}} = 9.2$ Hz, Ar–CH₂–N), 4.02 (m, 2H, Ar–O–CH₂–CH₂), 4.11 (m, 2H, Ar–O–CH₂), 4.21 (m, 2H, Ar–O–CH₂–CH₂), 4.22 (m, 2H, Ar–O–CH₂), 4.78 (q, 2H, $^3J_{\text{PH}} = 12.7$ Hz, $^2J_{\text{HH}} = 9.2$ Hz, Ar–CH₂–N), 6.95–7.28 (8H, Ar–H). ¹³C NMR (400 MHz, CDCl₃): δ 22.7 (*spiro* N–CH₂–CH₂), 26.3 ($^3J_{\text{PC}} = 9.0$ Hz, *pyrrolidine* N–CH₂–CH₂), 26.5 ($^3J_{\text{PC}} = 8.8$ Hz,

Table 1. Selected Bond Lengths (Å) and Angles (deg) with the Selected Torsion angles (deg) for **16** and **22**

16		22	
P3–N3	1.577(5)	P1–N1	1.6008(16)
P3–N2	1.585(4)	P1–N3	1.6287(16)
P3–N4	1.646(5)	P1–N4	1.6491(16)
P3–O1	1.596(4)	P1–N5	1.6324(16)
P1–N3	1.590(5)	P2–N1	1.5633(16)
P1–N1	1.586(4)	P2–N2	1.5804(16)
P1–N5	1.656(4)	P2–C11	1.9982(7)
P1–O2	1.569(4)	P2–C12	2.0097(7)
P2–N1	1.595(5)	P3–N2	1.5831(17)
P2–N2	1.604(4)	P3–N3	1.5525(15)
P2–N7	1.658(5)	P3–C13	2.0040(7)
P2–N6	1.651(4)	P3–C14	2.0173(7)
C1–N5–P1	117.4(4)	C1–N5–P1	113.76(13)
C9–N5–P1	113.8(3)	C19–N5–P1	123.72(13)
C1–N5–C9	111.5(4)	C19–N5–C1	117.92(15)
C2–N4–C10	120.4(5)	C3–N4–C4	112.10(16)
C2–N4–P3	122.6(5)	C3–N4–P1	115.51(12)
N3–P3–N2–P2	22.2(4)	N1–P1–N3–P3	–8.09(16)
N1–P2–N2–P3	8.9(4)	N2–P3–N3–P1	3.44(18)
N2–P2–N1–P1	–15.2(4)	N3–P3–N2–P2	5.47(17)
N3–P1–N1–P2	–9.6(4)	N1–P2–N2–P3	–9.26(17)
N1–P1–N3–P3	40.2(3)	N2–P2–N1–P1	4.28(17)
N2–P3–N3–P1	–47.0(3)	N3–P1–N1–P2	4.19(16)

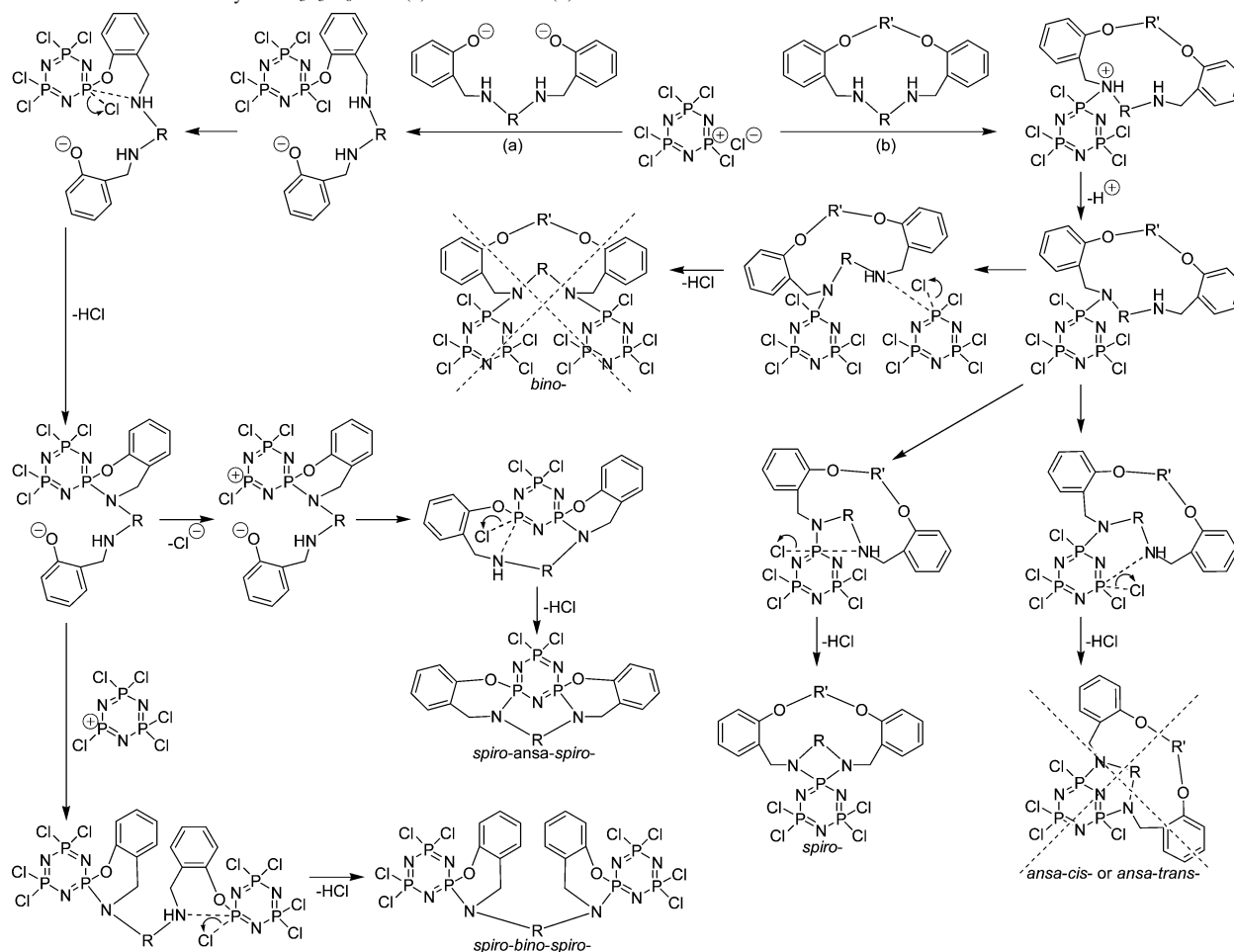
Table 2. Crystallographic Details

	16	22
empirical formula	C ₃₀ H ₄₀ N ₇ O ₆ P ₃	C ₁₉ H ₂₂ Cl ₄ N ₅ O ₂ P ₃
fw	687.60	587.13
cryst syst	monoclinic	orthorhombic
space group	<i>Cc</i>	<i>Pbca</i>
<i>a</i> (Å)	18.4420(11)	8.5470(3)
<i>b</i> (Å)	13.3370(9)	21.8940(11)
<i>c</i> (Å)	13.5691(14)	26.3773(10)
α (deg)	90.00	90.00
β (deg)	99.243(6)	90.00
γ (deg)	90.00	90.00
<i>V</i> (Å ³)	3294.1(5)	4935.9(4)
<i>Z</i>	4	8
μ (cm ⁻¹)	2.113 (Cu K α)	0.703 (Mo K α)
ρ_{calcd} (g cm ⁻³)	1.386	1.580
no. reflns total	3395	29107
no. reflns unique	3077	4830
R_{int}	0.029	0.083
$2\theta_{\text{max}}$ (deg)	148.50	52.08
$T_{\text{min}}/T_{\text{max}}$	0.5251/0.6202	0.7663/0.9204
no. params	416	330
$R1 [F^2 > 2\sigma(F^2)]$	0.0592	0.0281
wR2	0.1394	0.0653

pyrrolidine N–CH₂–CH₂), 45.9 (*spiro* N–CH₂), 46.2 ($^2J_{\text{PC}} = 3.8$ Hz, *pyrrolidine* N–CH₂), 46.3 ($^2J_{\text{PC}} = 3.2$ Hz, *pyrrolidine* N–CH₂), 46.7 (Ar–CH₂–N), 69.8 (Ar–O–CH₂), 70.2 (Ar–O–CH₂–CH₂), 114.8 (C₅), 121.0 (C₃), 127.9 (C₄), 130.0 ($^3J_{\text{PC}} = 11.6$ Hz, C₁), 130.5 (C₂), 151.5 (C₆).

X-ray Crystal Structure Determinations. Colorless crystals of **16** and **22** were grown by dissolving the compounds in hot *n*-heptane and allowing the solutions to cool slowly. Selected bond lengths and angles are given in Table 1, and crystallographic details are listed in Table 2. The crystallographic data were recorded on an Enraf Nonius CAD4 diffractometer using Cu K α radiation ($\lambda = 1.54184$ Å) at $T = 296$ K for **16** and a Stoe IPDS II diffractometer using Mo K α radiation ($\lambda = 0.71073$ Å) at $T = 100$ K for **22**. Absorption corrections by integration¹⁹ (for **22**) and ψ scan²⁰ (for **16**) were applied. Structures were solved by direct methods

(19) X-AREA, version 1.18; X-RED, version 1.04; Stoe & Cie: Darmstadt, Germany, 2002.

Scheme 2. Reaction Pathways of $N_3P_3Cl_6$ with (a) Podands and (b) Dibenzo-diaza-crown Ethers in THF

(SHELXS-97)²¹ and refined by full-matrix least squares against F^2 using all data (SHELXL-97).²¹ All non-H atoms were refined anisotropically. The H atom positions (H1A, H1B, H2A, H2B, H3A, H3B, H6, H7, H8, H9, H14, H15, H16, and H17 for **22** and all H atoms for **16**) were calculated geometrically at distances of 0.93 (CH) and 0.97 Å (CH₂) from the parent C atoms; a riding model was used during the refinement process, and the $U_{iso}(H)$ values were constrained to be 1.2 U_{eq} (carrier atom). The other H atoms were located in difference syntheses and refined isotropically for **22**.

Results and Discussion

Synthesis. Spiro-ansa-spiro-phosphazene **10** has been prepared by means of the reaction of $N_3P_3Cl_6$ with aminopodand **1**.^{8b} The fully substituted spiro-ansa-spiro-phosphazenes **14** and **16** were obtained by the reaction of **11** with an excess of pyrrolidine and DASD, respectively, in dry THF. Compounds **10** and **11** are the first examples of the ansa structure having an ethane-1,2-diamine precursor in contrast to the expectation of spiro structure, and their structures have previously been confirmed by X-ray crystallography.^{8b,8c} Interestingly, the P–N bonds of the seven membered ansa rings of **10** and **11** have cis configurations. Two P atoms of the ansa ring in **10** and **11** are stereogenic because they have

four different substituents. Therefore, they have R and S configurations (meso form). On the other hand, the reaction of the aminopodands (**2–4**) with $N_3P_3Cl_6$ in dry THF produces both spiro-ansa-spiro (**11–13**)^{8a} and spiro-bino-spiro (**17, 18**,^{8a} and **19**) architectures (Scheme 1) in different yields, depending on the chain lengths of aminopodands. The obtained yields can be given as follows: [spiro-ansa-spiro compound/spiro-bino-spiro compound]: 40 (**11**)/21% (**17**) for R = (CH₂)₂, 31 (**12**)/29% (**18**) for R = (CH₂)₃, and 18 (**13**)/52% (**19**) for R = (CH₂)₄. The reaction pathway is depicted in Scheme 2. If the chains are small, spiro-ansa-spiro derivatives are the major products, whereas, as the chain lengths increase, the yields of spiro-ansa-spiro products decrease. As shown in Scheme 2, this may be caused by the free rotation of long chains around the tertiary N atom bonded to the P atom. We have already described the synthesis and structures of spiro-crypta phosphazenes (**23** and **24**) which are the new families of macrocyclic multi-dentate ligands where the macrocycle and phosphazene rings are linked together, forming a novel structure by the reaction of $N_3P_3Cl_6$ with dibenzo-diaza-crown ethers (**7** and **8**).⁶ The novel spiro-crypta phosphazenes (**21, 22**, and **25**) have been obtained from the reactions of $N_3P_3Cl_6$ with the N₂O_x ($x = 2, 3$) donor-type dibenzo-diaza crown ethers (**5, 6**, and **9**), respectively. Since only the spiro arrangement is favored, in contrast to the various expectations (Scheme 2), the

(20) North, A. C. T.; Phillips, D. C.; Mathews, F. S. *Acta Crystallogr.* **1968**, *A24*, 351–359.

(21) Sheldrick, G. M. *SHELXS-97; SHELXL-97*; University of Göttingen: Göttingen, Germany, 1997.

Scheme 3. Possible Absolute Configurations of Geminal (gem) and Non-geminal (non-gem) Structures for Spiro-Crypta and Spiro-Ansa-Spiro-phosphazenes

Possibility	Configurations of nitrogen atoms	
	gem	non-gem
(i)		
³¹ P-NMR spin system	ABC, ABX or AMX	ABC, ABX or AMX
(ii)		
³¹ P-NMR spin system	AB ₂ , AM ₂ or AX ₂	A ₂ B, A ₂ M or A ₂ X
(iii)		
³¹ P-NMR spin system	ABC, ABX or AMX	ABC, ABX, AMX, A ₂ B, A ₂ M or A ₂ X

reactions of $N_3P_3Cl_6$ with the dibenzo-diaza crown ethers in THF are regioselective.

In **24**, the nitrogen atoms of the $ArCH_2N$ groups are stereogenic, and the configurations of N atoms are only RS on the basis of X-ray results^{6a} (Scheme 3, possibility i). Compounds **21** and **25** are also expected to show the same characteristics as **24**. Although several reports have recently appeared concerning the stereoisomerism of phosphorus atoms in phosphazene rings,^{2e,3b,9a,12} only a few reports about the stereoisomerism of the N atoms in phosphazene chemistry have been published by our group.^{6a,8b,8c} With an excess of pyrrolidine in THF, compounds **23** and **24** produce compounds **26** and **27**. The excess pyrrolidine was used as hydrochloride acceptor. In this reaction, the formation of the fully pyrrolidinyl-substituted phosphazenes $[N_3P_3(\text{macrocycle})(C_4H_7N)_4]$ was expected, but the major products isolated were the partially pyrrolidinyl-substituted geminal phosphazene derivatives $[N_3P_3(\text{macrocycle})(C_4H_7N)_2Cl_2]$, **26** and **27**. The chloride replacement reactions of phosphazene derivatives with pyrrolidine lead to the non-geminal reaction pathways.²² The reactions of phosphazene derivatives containing difunctional aromatic bulky diamines²³ and **11**, **12**, and **18**^{8a} with excess pyrrolidine gave only fully pyrrolidinyl-substituted products. The observation of the geminal substitution pathway (instead of the non-geminal) of **23** and **24** with excess pyrrolidine is unexpected and in contrast to the observations in the literature.²² Each $>PCl_2$ group sees different parts of the macrocycle, and the macrocycle hinders the attack of the

pyrrolidine nucleophile to one of the $>PCl_2$ groups. The geminal structure of **27** has been confirmed by X-ray structural analysis.²⁴ Elemental analyses, FTIR, CI- and ESI-MS, and NMR data are consistent with the proposed structures. The MS spectra of **10**, **16**, **19**, **21**, **22**, and **25–27** show protonated molecular ion $[M + H]^+$ peaks. In the spectrum of **14**, the molecular ion peak does not appear, but important fragments appear at m/z 530 and 516.

IR and NMR Spectroscopy. The FTIR spectra of phosphazene derivatives (**11**, **14**, **16**, **19**, **21**, **22**, and **25–27**) exhibit two medium intensity absorption bands at 3069–3059 and 3041–3025 cm^{-1} attributed to the asymmetric and symmetric stretching vibrations of the aromatic C–H groups. All phosphazenes display an intense band between 1238–1163 cm^{-1} corresponding to the $\nu_{P=N}$ of the phosphazene ring. Two kinds of $\nu_{P=N}$ absorption bands are seen for crypta phosphazenes (**21**, **22**, and **25**) at 1238–1229 and 1182–1163 cm^{-1} . The former values are larger than those of the spiro-ansa-spiro- and spiro-bino-spiro-phosphazenes (**10** and **19**, respectively). The characteristic ν_{N-H} stretching bands of the aminopodands and dibenzo-diaza-crown ethers disappear in the IR spectra of all the phosphazene derivatives. The absorption bands assignable to the stretching of PCl_2 bonds for the partially substituted phosphazenes (**10**, **19**, **21**, **22**, and **25–27**) were observed in the frequency range of 597–568 cm^{-1} .

The ¹H-decoupled ³¹P NMR spectral data of all of the phosphazene derivatives are listed in Table 3. According to the ¹H and ¹³C NMR spectral data of the compounds, all the molecules appear to have symmetric structures in the solution.

The expected spin systems of **21**, **22**, and **25** are likely to be AB₂ or AX₂, but the ³¹P NMR spectra of **21**, **25**, and **22** are interpreted as simple AMX and ABX spin systems, respectively. In **21**, **22**, and **25**, the $>PCl_2$ groups see different parts of the macrocycle. Therefore, they have different environments and show anisochrony (Figure 1) as observed for compounds **23** and **24**.^{6a} Compound **10** is another example that shows anisochrony in which the NPO phosphorus atoms possess different environments (Figure 1). But the analogous compound, **11**, having the same ethane-1,2-diamine precursor does not show anisochrony. The anisochronism of compound **10** may depend on the five-membered spiro-ring conformations. According to the X-ray crystallographic data of **10**,^{8b} five-membered spiro rings are nearly planar, but in **11**,^{8c} the six-membered spiro rings are not planar. In the literature,²⁵ it is claimed that anisochronism may depend on amine substituents containing stereogenic C atom bonded to phosphorus atom in the N_3P_3 ring. Anisochronism in phosphazene derivatives containing N atoms in exocyclic rings has been investigated by our group.^{6a} According to our findings, compound **23**⁶ showing anisochronism does not have stereogenic N atoms, but compound **11**^{8c} having stereogenic N atom does not show anisoch-

(22) (a) Alkubaisi, A. H.; Hursthouse, M. B.; Shaw, L. S.; Shaw, R. A. *Acta Crystallogr.* **1988**, *B44*, 16–22. (b) Lensink, C. L.; Ruiter B.; Grampel, J. C. *J. Chem. Soc., Dalton Trans.* **1984**, 1521–1526.
 (23) Bilge, S.; Özgüç, B.; Safran, S.; Demiriz, Ş.; İşler, H.; Havyalı, M.; Kılıç, Z.; Hökelek, T. *J. Mol. Struct.* **2005**, *748*, 101–109.

(24) Çaylak, N.; Hökelek, T.; Bilge, S.; Demiriz, Ş.; Kılıç, Z. *Anal. Sci.* Submitted.

(25) Vicente, V.; Fruchier, A.; Cristau, H. J. *Magn. Reson. Chem.* **2003**, *41*, 183–192.

Table 3. ^{31}P NMR Data (CDCl_3) of **10**–**27** (δ in ppm, J in Hz)

	spin system	δ_{PON}	$\delta_{\text{P(pyrr)}_2}$	δ_{PN_2}	δ_{PCl_2}	$^2J_{\text{PP}}$
10	ABC	P_{B} 36.50 P_{C} 36.53			P_{A} 34.72	$^2J_{\text{BC}} \sim 0$ $^2J_{\text{AC}}$ 65.9 $^2J_{\text{AB}}$ 87.3
11 ^{8a}	A ₂ X	P_{A} 19.59			P_{X} 29.35	$^2J_{\text{AX}}$ 70.1
12 ^{8a}	A ₂ X	P_{A} 15.95			P_{X} 32.28	$^2J_{\text{AX}}$ 69.4
13 ^{8a}	A ₂ X	P_{A} 15.83			P_{X} 32.28	$^2J_{\text{AX}}$ 69.4
14	A ₂ B	P_{A} 20.15	P_{B} 24.10			$^2J_{\text{AB}}$ 53.5
15 ^{8a}	A ₂ B	P_{A} 20.68	P_{B} 23.42			$^2J_{\text{AB}}$ 55.7
16 ^a			~ 23.50			
17 ^{8a}	AX ₂	P_{A} 6.56			P_{X} 25.10	$^2J_{\text{AX}}$ 56.1
18 ^{8a}	AX ₂	P_{A} 6.78			P_{X} 25.09	$^2J_{\text{AX}}$ 55.7
19	AX ₂	P_{A} 5.75			P_{X} 23.89	$^2J_{\text{AX}}$ 56.2
20 ^{8a}	AB ₂ A'B' ₂	P_{A} 18.89 $P_{\text{A}'}$ 18.92	P_{B} 20.38 $P_{\text{B}'}$ 20.39			$^2J_{\text{AB}}$ 46.6 $^2J_{\text{A'B'}}$ 47.0
21	AMX			P_{A} 14.56	P_{M} 21.03 P_{X} 24.33	$^2J_{\text{AM}}$ 47.0 $^2J_{\text{AX}}$ 47.3 $^2J_{\text{MX}}$ 75.8
22	ABX			P_{A} 14.20	P_{B} 17.51 P_{X} 22.72	$^2J_{\text{AB}}$ 21.5 $^2J_{\text{AX}}$ 57.6 $^2J_{\text{BX}}$ 58.0
23 ^{6a}	AMX			P_{A} 15.50	P_{M} 23.58 P_{X} 25.46	$^2J_{\text{AM}}$ 31.4 $^2J_{\text{AX}}$ 54.0 $^2J_{\text{MX}}$ 78.8
24 ^{6a}	ABX			P_{A} 17.15	P_{B} 19.58 P_{X} 23.50	$^2J_{\text{AB}}$ 65.2 $^2J_{\text{AX}}$ 65.5 $^2J_{\text{BX}}$ 65.4
25	AMX			P_{A} 14.46	P_{M} 19.35 P_{X} 21.56	$^2J_{\text{AM}}$ 48.0 $^2J_{\text{AX}}$ 42.3 $^2J_{\text{MX}}$ 71.6
26	ABX		P_{A} 12.88	P_{B} 14.08	P_{X} 23.32	$^2J_{\text{AB}} \sim 0$ $^2J_{\text{AX}}$ 43.4 $^2J_{\text{BX}}$ 59.3
27	AMX	-	P_{A} 14.75	P_{M} 19.95	P_{X} 22.87	$^2J_{\text{AM}}$ 55.7 $^2J_{\text{AX}}$ 38.3 $^2J_{\text{MX}}$ 16.0

^a Chemical shifts overlap.

ronism. Therefore, it is concluded that there is no connection between stereogenicity and anisochronism. The reaction of dibenzo-diaza-crown ethers and aminopodands with $\text{N}_3\text{P}_3\text{Cl}_6$ give geminal-disubstituted spiro-crypta and non-geminal-disubstituted spiro-ansa-spiro-phosphazenes with three possibilities according to nitrogen atoms (Scheme 3). It is clear that one can easily verify the absolute configurations of N atoms in spiro-crypta and spiro-ansa-spiro-phosphazenes from the spin systems of ^{31}P NMR spectra. The experimental AMX and ABX types of spectra of **21**, **25**, and **22** are, respectively, in accordance with R/S(S/R)- and R(S) configurations of possibilities i and iii. On the other hand, according to X-ray data, there is only one stereogenic N atom in spiro-ansa-spiro derivatives **10** (ABX), **11** (A₂X spin system),^{8a} and **16**. Moreover, the coupling constants between the two $>\text{PCl}_2$ groups of anisochronic derivatives can be estimated from the non-first-order spectrum. Taking into account the $^2J_{\text{PP}}$ values in the anisochronic spiro-crypta phosphazenes, we conclude that if the $^2J_{\text{PP}}$ values are nearly the same, either two nitrogen atoms in the macroring have pyramidal geometry (stereogenic), two of the $^2J_{\text{PP}}$ values are nearly the same, one nitrogen atom has pyramidal geometry, or all three of the $^2J_{\text{PP}}$ values are different, no nitrogen atom has pyramidal geometry. In addition, it is interesting that the $^2J_{\text{PP}}$ value between the PN_2 and P(pyrr)_2 atoms in **26** is very close to zero; therefore, the signals of P(pyrr)_2 and PN_2 are *doublet* instead of *quartet*. Compound **14** shows a typical

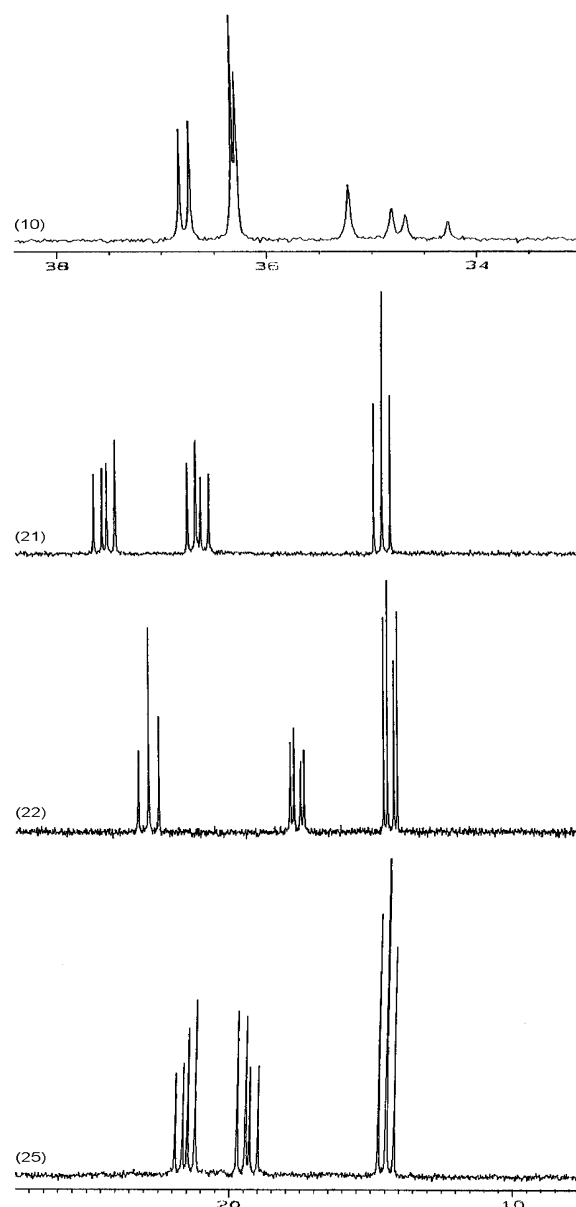


Figure 1. Anisochronism of spiro-ansa-spiro- (**10**) and spiro-crypta (**21**, **22**, and **25**) phosphazenes.

five-line resonance pattern consisting of a *doublet* for two PON atoms in the spiro-ansa-spiro ring and a *triplet* for one P(pyrr)_2 atom. The signal of dipyrrolidinyl-substituted P atom of **14** is upfield-shifted by 5.25 ppm with respect to the corresponding PCl_2 atom of **11**. The δ_{P} shifts of **16** accidentally overlap centering at $\delta \approx 23.50$ ppm. The ^{31}P NMR spectra of **19** consists of a *triplet* and a *doublet* which are assigned to the two spiro atoms (PON) and the four PCl_2 atoms, and the signals of **19** are upfield-shifted, compared to those of **14**. Consequently, according to the signal patterns in the ^{31}P NMR spectra of the phosphazene derivatives, it can easily be determined whether the phosphazenes prepared by the reaction of aminopodand (**2**–**4**) with $\text{N}_3\text{P}_3\text{Cl}_6$ have the spiro-ansa-spiro (**11**–**13**)^{8a} or spiro-bino-spiro (**17**, **18**,^{8a} and **19**) architectures.

The bond angles (α , α' , β , γ , γ' , and δ) of the phosphazene derivatives are given in Table 4. The variations in the bond

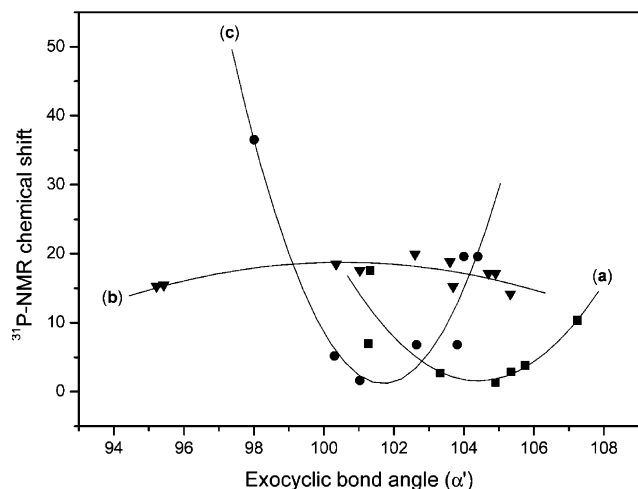


Figure 2. Plot of δP shifts against the exocyclic bond angles (α') of (a) spirocyclic phosphaza (PNP) lariat ethers (■), (b) spiro-crypta phosphazenes (▼), and (c) spiro-ansa-spiro-, spiro-bino-spiro-, and spiro-phosphazenes (●).

a and b show contrasting trends in Figure 2. In Figure 2b, it was observed that the points of the five- and six-membered rings of the spiro-crypta phosphazenes were accumulated on the left- and right-hand sides of the curve, respectively. Figure 2c was also drawn for OPN (α') bond angles versus the δP shifts of spiro-ansa-spiro- (**10** and **11**), spiro-bino-spiro- (**18**), and spiro-phosphazene derivatives (**I** and **II**) (Table 4) taken from the literature.^{28,30,31} The trend observed for the α' angles (Figures 2a and 2c) is in good correlation with that of Shaw.²⁶ Moreover, a linear trend has been observed between δP_{spiro} shifts and the endocyclic NPN bond angles for a series of analogous spiro-phosphazene derivatives by Labarre.³² We have also investigated the relationship between the δP shifts and the endocyclic NPN (α) angles. We compared three groups of compounds in Figure 3: (a) spirocyclic phosphaza lariat ethers^{7a,7c,23} (Table 4), (b) Labarre compounds taken from the literature,³² and (c) spiro-crypta phosphazenes (**23**, **24**, and **27** and four analogous compounds,^{28,29} Table 4). Linearity between the δP_{spiro} shift and the endocyclic α angle is observed for spirocyclic phosphaza lariat ethers. As can be seen from Figure 3, H_3PO_4 (the standard compound which possesses a pseudo-tetrahedral structure) fits the relationships, supporting the validity of the equations given as follows: $\alpha = 0.9862\delta P + 111.00$ ($R = 0.93$) for Figure 3a and $\alpha = 0.2732\delta P + 109.67$ ($R = 0.97$) for Figure 3b. However, for spiro-crypta phosphazenes, it seems to be a “cluster” of points rather than a trend of the linearity. The δP_{spiro} shift and α value for the spirocyclic phosphaza lariat ether (**VII**)^{23,27} (Table 4) have not been taken into account in Figure 3a because the point of **VII** significantly deviates from the linear trend (experimental and

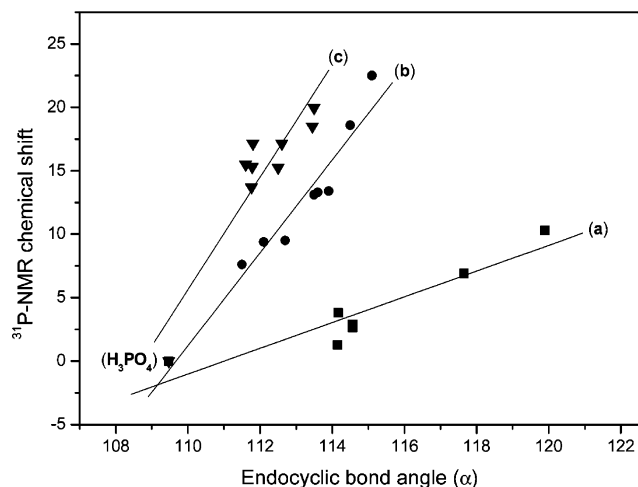


Figure 3. Plot of the δP shifts against the endocyclic bond angles (α) of (a) spirocyclic phosphaza (PNP) lariat ethers (■), (b) Labarre compounds taken from the literature³² (●), and (c) spiro-crypta phosphazenes (▼) (H_3PO_4 , 109.47° , $\delta P = 0.00$ ppm).

calculated values are $117.60(14)$ and 128.33° , respectively). The deviation may be caused by the packing in its unit cell, exhibiting strong intra- and intermolecular contacts. Indeed, the trends which exist between the ^{31}P NMR and X-ray data allow prediction of the α angles. However, solvent interactions alter the δP shifts, while the intra- and intermolecular contacts in the unit cell affect the α angles. Consequently, the results become more reliable when the NMR measurements and X-ray data are taken into account.

The ^1H NMR spectra of **14** and **16** indicate that all of the chlorine atoms in **11** have been substituted by pyrrolidine and DASD, respectively. On the other hand, in the fully substituted derivatives **14** and **16**, the NCH_2CH_2 and NCH_2 proton signals of the pyrrolidine and DASD rings are easily distinguished from those of the ansa rings by the HETCOR spectra of these compounds, respectively. The ArCH_2N benzylic protons of **14** and **16** are separated from each other at 3.84 and ~ 4.47 ppm, as *quartets*, in which they have three bond-coupling constants, $^3J_{\text{PH}} \approx 15.0$ Hz. The protons of the benzylic moieties give rise to *quartet* or *multiplet* for spiro-ansa-spiro derivatives (**14** and **16**) and to *doublet* for the spiro-bino-spiro (**19**) derivatives, probably, because of the higher flexibility of the spiro-bino-spiro-phosphazene. Generally, the geminal $-\text{CH}_2-$ protons are not equivalent to each other for spiro-crypta phosphazenes (**21**, **22**, and **25–27**); therefore, the spectra of the compounds show complex signals upon the preference of diastereotopic groups. Interestingly, the peaks of ArCH_2N protons of the spiro-crypta phosphazenes are highly separated from each other, as in the spiro-ansa-spiro-phosphazenes (**14** and **16**). These protons are observed at 3.28–3.95 and 4.57–4.78 ppm as two groups of *quartets* because of the geminal proton couplings ($^2J_{\text{HH}}$) and the three bond-couplings ($^3J_{\text{PH}}$). In addition, the C atoms and the geminal protons of $\text{ArOCH}_2\text{CH}_2$ and ArOCH_2 are also distinguishable from the HETCOR spectra. The HETCOR spectrum of **25** is depicted in Figure 4 as an example. One can notice that the order of the ^{13}C shifts for the ArOCH_2 and $\text{ArOCH}_2\text{CH}_2$ groups are different from those of ^1H shifts.

(29) (a) Tercan, B.; Hökelek, T.; Büyükgüngör, O.; Asmafiliz, N.; Ilter, E. E.; Kılıç, Z. *Acta Crystallogr.* **2005**, *E61*, 2145–2147. (b) Asmafiliz, N.; Ilter, E. E.; Işıklan, M.; Kılıç, Z.; Tercan, B.; Çaylak, N.; Hökelek, T.; Büyükgüngör, O. *J. Mol. Struct.* Submitted. (c) Asmafiliz, N. G. Master Dissertation, Ankara University, Ankara, Turkey, 2005.

(30) Dal, H.; Safran, S.; Süzen, Y.; Hökelek, T.; Kılıç, Z. *J. Mol. Struct.* **2005**, *753*, 84–91.

(31) Tercan, B.; Hökelek, T.; Işıklan, M.; Ilter, E. E.; Kılıç, Z. *Acta Crystallogr.* **2004**, *E60*, 971–973.

(32) Labarre, M. C.; Labarre, J. F. *J. Mol. Struct.* **1993**, *300*, 593–606.

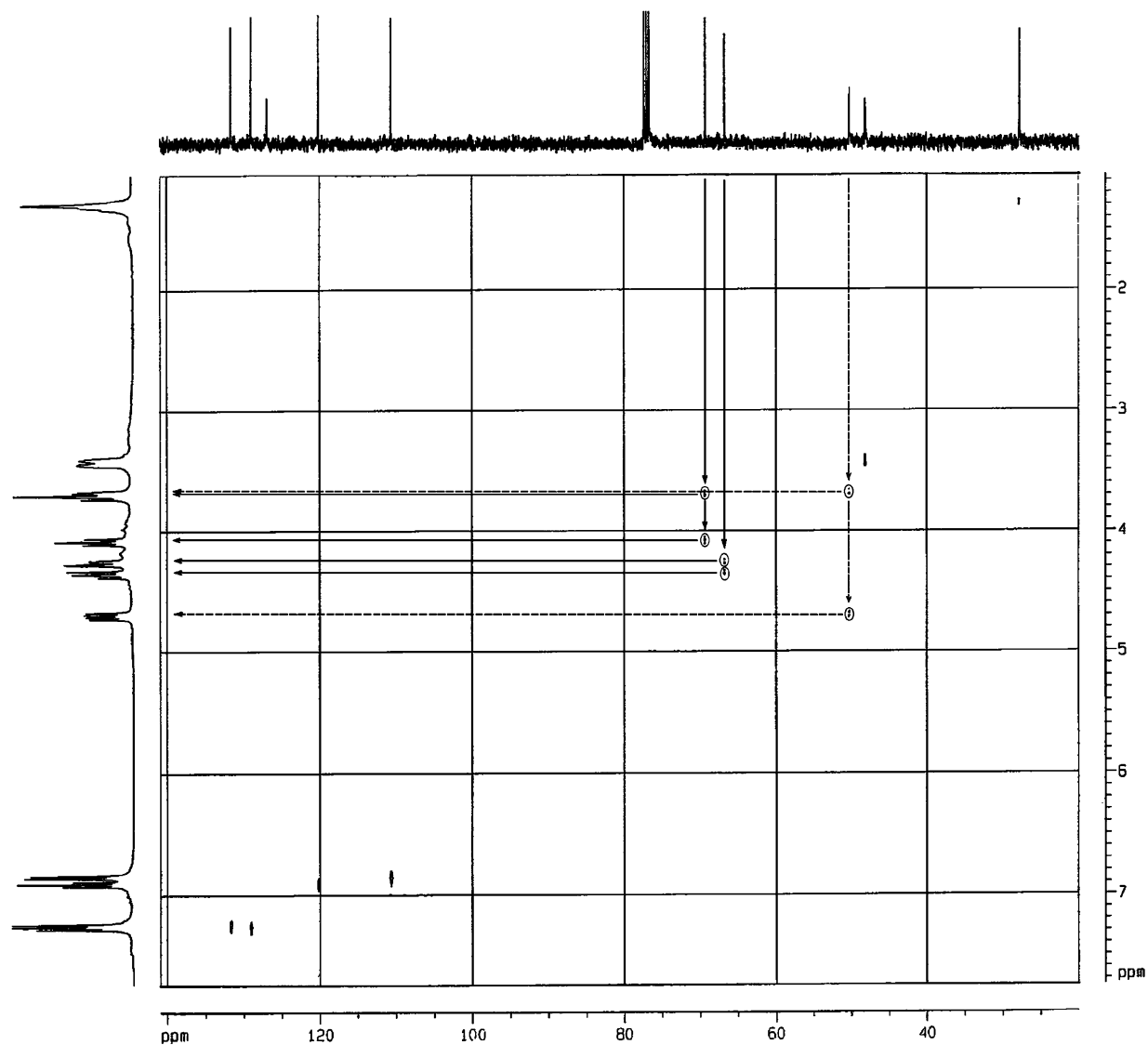


Figure 4. HETCOR NMR spectrum (400 MHz) of **25**. The dashed line (---) indicates ArCH₂N and the solid line (—) indicates the ArOCH₂CH₂ and ArOCH₂ groups.

The NCH₂ signals of the ansa rings of **14** and **16**, which were confirmed by HETCOR experiments, are distinguished from NCH₂ carbon signals of pyrrolidine and DASD precursors, respectively. Two different NCH₂CH₂ and NCH₂ signals of the pyrrolidine and DASD precursors are observed for **14** and **16**. In the spiro-ansa-spiro- (**14**) and spiro-bino-spiro-phosphazenes (**19**), the couplings expected between the aromatic carbon and phosphorus atoms were observed for the C₁, C₅, and C₆ carbons (Scheme 1) (not observed for **16**). These couplings (³J_{PC1}, ³J_{PC5}, and ²J_{PC6}) have been observed as *triplets* for (**14**) and *doublets* for (**19**), as observed in the analogous compounds (**11–13** and **15** and **17, 18**, and **20**).^{8a} The *triplets* have also been observed for the aliphatic N–CH₂ carbons of **10** because of the second-order effects,^{8a,23} which estimate the J_{PC} coupling constants between the external transitions of the *triplets*.²⁵ The ²J_{PC} value of NCH₂ for the spiro-crypta phosphazenes, which have five-membered spiro rings, are found to be very large. In addition, the coupling constants (²J_{PC}) of the spiro-crypta phosphazenes are in the following order: five-membered

spiro rings (**21, 23**,^{6a} and **26**) > seven-membered spiro ring (**25**) > six-membered spiro rings (**24**^{6a} and **27**).

X-ray Structures of 16 and 22. The X-ray structural determinations of compounds **16** and **22** confirm the assignments of their structures from spectroscopic data. The molecular structures of **16** and **22** along with the atom-numbering schemes are depicted in Figures 5 and 6, respectively. The phosphazene rings of **16** and **22** are not planar and are in twisted boat forms [Figure 7a $\varphi_2 = -70.0(4)^\circ$ and $\theta_2 = 68.9(4)^\circ$; Figure 8a $\varphi_2 = 155.5(8)^\circ$ and $\theta_2 = 87.7(8)^\circ$] having total puckering amplitudes,³³ Q_T , of 0.439(3) and 0.107(1) Å, respectively.

In **16**, the six-membered rings (P3/N4/C10/C11/C16/O1) and (P1/N5/C9/C8/C3/O2) are in twisted forms with total puckering amplitudes, Q_T , of 0.459(4) and 0.515(4) Å, respectively. In addition, the six-membered rings, N7/C22/C23/C24/C25/C26 and N6/C17/C18/C19/C20/C21, of the DASD moieties in **16** have chair conformations with total

(33) Cremer, D.; Pople, J. A. *J. Am. Chem. Soc.* **1975**, *97* (6), 1354–1358.

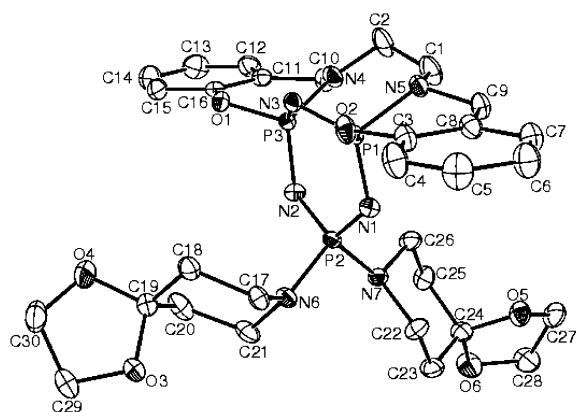


Figure 5. An ORTEP-3⁴² drawing of **16** with the atom-numbering scheme. Displacement ellipsoids are drawn at the 50% probability level.

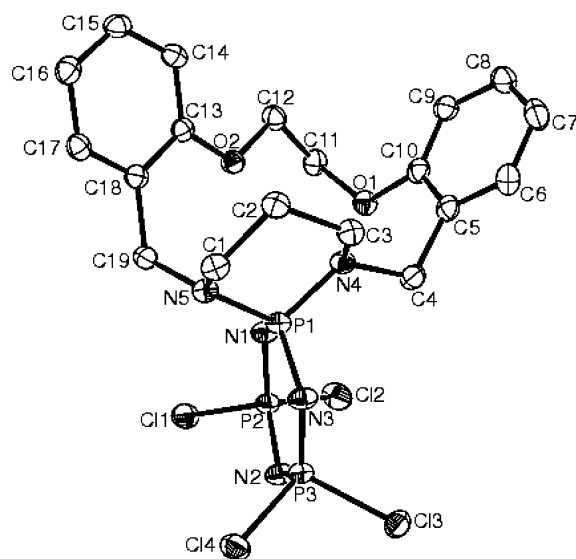


Figure 6. An ORTEP-3⁴² drawing of **22** with the atom-numbering scheme. Displacement ellipsoids are drawn at the 50% probability level. puckering amplitudes, Q_T , of 0.550(6) and 0.581(7) Å, respectively. The bicyclic system made up of phosphazene and the ansa (P1/N3/P3/N4/C2/C1/N5) precursor is in the sofa conformation, which resembles the stable “adamantane” structure, where each ring is in a V shape (Figure 7a). The dihedral angle between the best least-squares planes of P1/N1/P2/N2/P3 and P1/P3/N4/N5 is 62.9(1)°, and it can be compared with the reported values of 62.2(2)° and 62.3(2)° in the bicyclic phosphazene [N₄P₄(NC₄H₈)₅(NH^mPr)(NⁿPr)]³⁴ and 68.0(2)° in the spiro-ansa-spiro-phosphazene skeleton (**11**).^{8c} In the bicyclic systems, the maximum separations between the P and C atoms are [P2⋯C1 = 4.141(3) Å and P2⋯C2 = 4.451(3) Å]. All the P⋯P distances are in the range of 2.643(2)–2.779(2) Å.

In **22**, the six-membered ring (P1/N5/C1/C2/C3/N4) is in chair conformation [Figure 8b $Q_T = 0.657(2)$ Å, $\varphi_2 = 26.2(2)^\circ$, and $\theta_2 = 94.0(2)^\circ$], and phosphazene ring has a pseudo-2-fold axis running through atoms N1 and P3, as can be deduced from torsion angles (Table 1). As expected, the macrocyclic ring is not planar with the puckering amplitude, Q_T , of 2.682(2) Å.

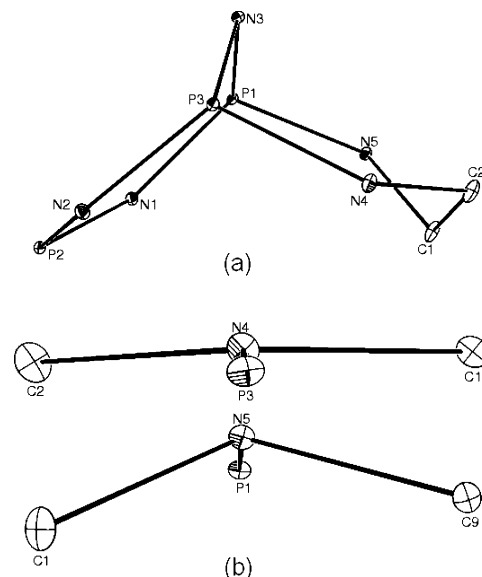


Figure 7. (a) Conformation of the bicyclic system and (b) the configurations of the spirocyclic N atoms in **16**. The substituents have been omitted for clarity.

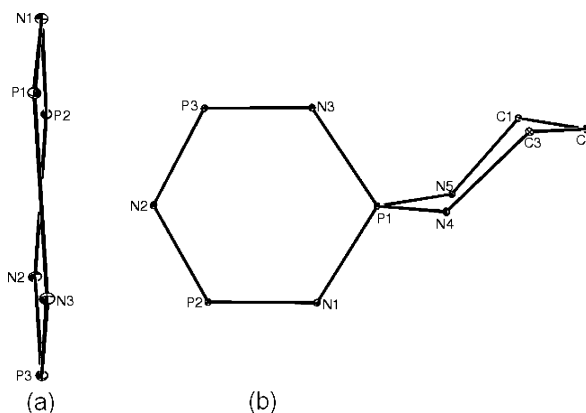


Figure 8. Conformations of (a) the phosphazene and (b) the six-membered spiro ring in **22**.

The average P–N bond lengths in phosphazene rings of **16** and **22** are 1.590(4) and 1.585(2) Å, which are shorter than the average exocyclic P–N bonds of 1.636(5) and 1.641(2) for **16** and **22**. The electron back-donation also causes the shortening of the exocyclic P–N bonds according to the average P–N single bond of 1.683(5) Å.³⁵

As can be seen from Table 4, in **22**, the α angle is narrowed, while the α' and β angles are expanded, considerably, according to the “standard” compound N₃P₃Cl₆. In N₃P₃Cl₆, the α , α' , and β angles are 118.3(2), 101.2(1), and 121.4(3)°, respectively.³⁶ On the other hand, in **10**,^{8b} **11**,^{8c} and **16**, the δ angles [114.5(2), 114.1(3), and 113.2(3)°, respectively, Table 4] have unexpectedly small values with respect to the corresponding ones in the spiro-crypta phosphazenes and N₃P₃Cl₆, probably because of the conformations of the bicyclic rings in the spiro-ansa-spiro-phosphazenes (Figure 7a).

The sums of the bond angles around atoms N4 and N5 [359.5(5) and 342.7(4)° for **16** and 344.8(1)° and 355.4(14)

(34) Öztürk, L.; Işıklan, M.; Kılıç, Z.; Hökelek, T. *Acta Crystallogr.* **2002**, C58, 80–83.

(35) Allen, F. H.; Kennard, O.; Watson, D. G.; Brammer, L.; Orpen, A. G.; Taylor, R. *J. Chem. Soc., Perkin Trans. 2* **1987**, 1–19.

(36) Bullen, G. J. *J. Chem. Soc. A* **1971**, 1450–1453.

for **22**] show a change in the hybridization of N5 atom for **16** and N4 atom for **22** from trigonal planar toward pyramidal. Thus, the N5 atom for **16** and the N4 atom for **22** may represent stereogenic centers (Scheme 3, possibility iii). The N atom with pyramidal geometry might be expected to give rise to optical activity (chirality) if the N atom was connected to three different groups, since the unshared pairs of electrons are analogous to the fourth group. This kind of chirality is merely a result of the acyclic tervalent chiral N atom. For the cyclic molecules in which the N atom is at a bridgehead, pyramidal inversion is prevented.³⁷ Tröger's base is one of the oldest examples of this kind of optically active compound.³⁸ Moreover, atoms P1 and P3 for **16** each have different attachments and thus are also expected to be stereogenic centers in the solid state. They have R and S configurations (meso forms). The Flack absolute structure parameter³⁹ of **16** was refined; the expected values are 0 for the correct and +1 for the inverted absolute structure. The refined value is 0.08(6). So, the absolute structure is determined reliably. If we have the correct absolute structure, then we can correctly assign the chiral center. The absolute configuration of the chiral nitrogen center (N5) in compound **16** can be designated as S, indicating that the Cahn–Ingold–Prelog (CIP)⁴⁰ priority order of groups is $\text{PN}_3 > \text{CH}_2\text{Ph} > \text{CH}_2\text{CH}_2$.

The inner-hole size of the macrocycle in the radii of **22** was estimated to be twice the mean distance of the donor atoms from their centroids and is approximately 1.27 Å, using the “modified covalent radii” of the N_{sp^3} (0.72 Å) and O_{sp^3} (0.76 Å) atoms as in the literature method.⁴¹

Conclusions

Two different novel spiro-bino-spiro- (**19**) and spiro-crypta (**21**, **22**, and **25**) phosphazene derivatives have been synthe-

sized via the condensation reactions of $\text{N}_3\text{P}_3\text{Cl}_6$ with aminopodand (**4**) and dibenzo-diaza-crown ethers (**5**, **6**, and **9**). The substitution reactions of partially substituted phosphazene derivatives (**11**, **23**, and **24**) with pyrrolidine and DASD have also been investigated. The correlations of the δP shifts with the exocyclic α' angles of spiro-crypta, spiro-ansa-spiro-, spiro-bino-spiro-phosphazenes and the endocyclic α angles of the spiro-crypta phosphazenes and spirocyclic phosphazene lariat ethers (Table 4) have been discussed. The variations of the δP shifts depend essentially on the variations of the angles around the phosphorus atoms and presumably on the change of the α and α' angles. The trends between the ^{31}P NMR and the X-ray data allow the prediction of α angles by the δP shifts. Interestingly, the ^{31}P NMR spectra of **21**, **22**, and **25** show that the $>\text{PCl}_2$ groups of the compounds have anisochrony. The results obtained from the ^{31}P NMR and X-ray data indicate that there are no direct relationships between stereogenicity and anisochronism. Further studies in this direction are currently underway.

Acknowledgment. The authors acknowledge the purchase of the CAD-4 diffractometer and other financial supports under grants DPT/TBAG1 of the Scientific and Technical Research Council of Turkey, The faculty of Arts and Sciences, Ondokuz Mayıs University, Turkey, for the use of the STOE IPDS II diffractometer (purchased under Grant F.279 of the University Research Fund), Ankara University Research Fund (Grant 20050705107) and Hacettepe University, Scientific Research Unit (Grant 02 02 602 002) are also acknowledged.

Supporting Information Available: Additional figures giving crystal packing diagrams and X-ray crystallographic files in CIF format for compounds **16** and **22**. This material is available free of charge via the Internet at <http://pubs.acs.org>.

IC060630N

- (37) (a) Hökelek, T.; Akduran, N.; Bilge, S.; Kılıç, Z. *Anal. Sci.* **2001**, *17*, 465–466. (b) Bilge, S. Ph.D. Dissertation, Ankara University, Ankara, Turkey, 2005.
 (38) March, J. *Advanced Organic Chemistry: Reactions, Mechanisms and Structure*, 4th ed.; John Wiley & Sons: New York, 1992; Chapter 4.
 (39) Flack, H. D. *Acta Crystallogr.* **1983**, *A39*, 876–881.
 (40) Cahn, R. S.; Ingold, C. K.; Prelog, V. *Pure Appl. Chem.* **1976**, *45*, 10–30.

- (41) (a) Goodwin, H. J.; Henrick, K.; Lindoy, L. F.; McPartlin, M.; Tasker, P. A. *Inorg. Chem.* **1982**, *21*, 3261–3264. (b) Hökelek, T.; Akduran, N.; Bilge, S.; Kılıç, Z. *Anal. Sci.* **2001**, *17*, 801–802. (c) Hökelek, T.; Bilge, S.; Akduran, N.; Kılıç, Z. *Cryst. Res. Technol.* **2001**, *36* (3–4), 509–515. (d) Hökelek, T.; Bilge, S.; Kılıç, Z. *Acta Crystallogr.* **2003**, *E59*, 1607–1609.
 (42) Farrugia, L. J. *J. Appl. Crystallogr.* **1997**, *30*, 565.